Reduced interface roughness scattering in InGaAs/InAlAs quantum cascade lasers grown on (411)A InP substrates

M. P. Semtsiv, S. S. Kurlov, D. Alcer, Y. Matsuoka, J.-F. Kischkat, O. Bierwagen, and W. T. Masselink

Citation: Appl. Phys. Lett. **113**, 121110 (2018); doi: 10.1063/1.5049090
View online: https://doi.org/10.1063/1.5049090
View Table of Contents: http://aip.scitation.org/toc/apl/113/12
Published by the American Institute of Physics

Reduced interface roughness scattering in InGaAs/InAlAs quantum cascade lasers grown on (411)A InP substrates

M. P. Semtsiv,[1,a)] S. S. Kurlov,[1] D. Alcer,[1] Y. Matsuoka,[1] J.-F. Kischkat,[1] O. Bierwagen,[2] and W. T. Masselink[1]

[1]*Department of Physics, Humboldt University Berlin, Newtonstrasse 15, D-12489 Berlin, Germany*
[2]*Paul-Drude-Institut für Festkörperelektronik, Leibniz-Institut im Forschungsverbund Berlin e. V., Hausvogteiplatz 5-7, 10117 Berlin, Germany*

(Received 19 July 2018; accepted 6 September 2018; published online 19 September 2018)

Lattice-matched InGaAs-InAlAs quantum cascade lasers were prepared to compare differences between using a (411)A InP substrate and a (100) InP substrate. The lasers grown on the (411)A substrate showed higher gain, lower threshold current density, higher slope efficiency, and twice the power efficiency compared to the otherwise-identical structure on the (100) substrate. This performance improvement is attributed to less interface roughness scattering at the heterointerfaces in the (411)A structure. The lower interface roughness scattering appears to result from the high-spatial frequency steps on the (411)A surface. *Published by AIP Publishing.*
https://doi.org/10.1063/1.5049090

Since its first demonstration in 1994,[1] the Quantum-Cascade Laser (QCL) has been steadily developed into a laser suited for many applications in the mid-infrared. Besides the wide range of emission wavelengths available today and high-temperature performance with continuous-wave operation above 400 K,[2,3] room-temperature power efficiency has been dramatically improved from much less than 1% to now approaching the expected limit of near 30%.[4–8] More power and better power efficiency remain, however, important goals for further research. Regardless of how well optimized a QCL structure's design is, there are two processes that limit efficiency: inelastic longitudinal-optical (LO)-phonon assisted scattering and elastic interface-roughness (IFR) assisted scattering.[9–13] Both of these processes degrade efficiency both by mediating non-radiative transitions from the upper laser level into the lower laser level and by mediating scattering out of the upper laser level into higher confined states. The LO-phonon scattering is driven by temperature and can be minimized through clever engineering of the higher-lying states and through thermal management. It can also be altered by breaking of the continuous energy dispersion in high magnetic fields.[9,14,15] The IFR scattering can be reduced by reducing the product of conduction band offset and the electron probability at interfaces[16] and by reducing the interface roughness through optimized epitaxial growth.[17]

In this paper, we focus on interface roughness scattering and how to effectively reduce it in QCLs. Interface roughness is characterized by two parameters, Δ and Λ, where Δ is a measure of the roughness amplitude perpendicular to the plane of the interface and Λ describes the lateral extent of the fluctuations.[18] The energy difference of the conduction band minimum at the interface, δU, is also important, prompting the idea to use low-δU interfaces where the wavefunctions are peaked.[16] The IFR mediates scattering of electrons out of the upper laser level into both higher lying bands and into the lower laser level.[19] The scattering rate between the upper laser state u and the lower laser state l is equal to

$$R_{u,l} = \frac{\pi m_c}{\hbar^3}\Delta^2\Lambda^2\delta U^2\eta\exp(-\Lambda^2 q^2/4), \tag{1}$$

where δU is the conduction band discontinuity and q is the wavevector through which the electron is scattered. m_c is the electron effective mass in the conduction band, and the parameter $\eta = \sum_i |\varphi_u(z_i)\varphi_l(z_i)|^2$ is the product of electron probabilities summed over all interfaces. Reference 20 gives more accurate expression for $R_{u,l}$ including the Boltzmann distribution of carriers at elevated temperatures; this more accurate treatment results in almost the same position of the maximum and a very similar shape of $R_{u,l}$ at room temperature, so we will use Eq. (1) in this paper for simplicity.

As it is seen from Eq. (1), the interface roughness scattering is low if either $q\Lambda \gg 1$ or $q\Lambda \ll 1$ and has a maximum for $q\Lambda = 2$. Thus, IFR with either high spatial frequency or very low spatial frequency results in much less IFR scattering and that a reduction in IFR scattering can be accomplished by reducing interface roughness with $\Lambda \approx 2/q$. Depending on the value of momentum transfer q, the lateral size of dominant IFR ranges between a few nm and a few tens of nm.

Although it is difficult to obtain the Λ parameter directly from experiment, the product $\Delta\Lambda$ is more readily measured and has been determined to be in the range of 0.6–1.2 nm^2 for InGaAs/InAlAs interfaces.[9,16,21–23] Reference 21 quotes values of $\Lambda = 6$ nm and $\Delta = 0.17$ nm for the InGaAs/InAlAs interface grown on a (100) InP substrate by MBE. Somewhat lower $\Delta = 0.115$ nm and larger $\Lambda = 10.0$ nm are deduced from performance analysis of MOVPE grown QCLs.[23] While Ref. 17 shows that the Λ parameter can be anything between 5.5 nm and 18.5 nm depending on the MBE growth temperature. Figure 1 depicts the intersubband interface roughness scattering rate calculated using Eq. (1) for three different QCL emission wavelengths ($\lambda = 4$, 9, and 20 μm) as functions of lateral roughness size Λ for a fixed value of

a)Author to whom correspondence should be addressed: semtsiv@physik.hu-berlin.de

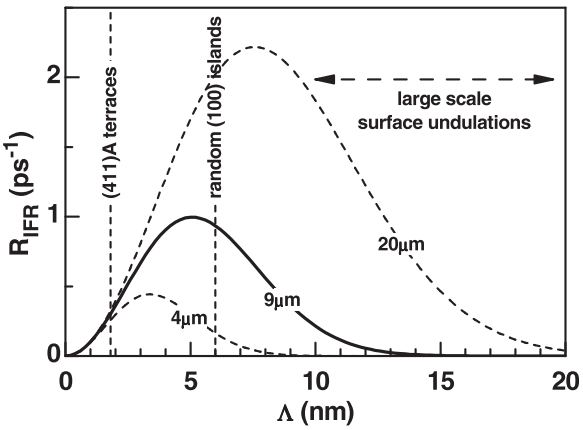

FIG. 1. Intersubband interface roughness scattering rate calculated for three different emission wavelengths ($\lambda = 4$, 9, and 20 μm) as functions of lateral roughness size Λ for a fixed value of $\Delta = 0.17$ nm, $\eta = 0.005\,\text{nm}^{-2}$, $m_c = 0.043m_0$, and $\delta U = 520$ meV.

$\Delta = 0.17$ nm. As we see, the value of $\Lambda = 6$ nm quoted in Ref. 21 results in nearly the highest scattering rates for QCLs emitting in the spectral range between 9 and 20 μm. Therefore, any substantial change of the lateral morphology of the interfaces should lead to improvement in QCL performance for this spectral range.

Commonly used methods for achieving an almost atomically flat epitaxial growth front include growth at high temperatures, the use of growth interruptions, and optimization of the III/V ratio. Another method to achieve smoother interfaces which has not yet been used in QCLs is the use of off-cut substrates. The off-cut substrates introduce monolayer-high steps into the growth front, but these steps are more regular than the random monolayer-high islands on the exact (100) surface, and are characterized by a different lateral size Λ. Growth proceeds in the step-flow mode, reducing fluctuations with random lateral extent. One of the common off-cuts in zincblende substrates is the (411)A orientation; this orientation is equivalent to a (100) orientation that is tilted by 19.5° in the [011] direction. (411)A oriented substrates are known to support a very flat surface morphology during the epitaxy with 1.8 nm long terraces along the $[\bar{1}, 2, 2]$ direction on InP,[24] which is much shorter than the $\Lambda = 6$ nm, quoted for the random fluctuations in InGaAs/InAlAs interfaces grown on the exact (100) InP substrate. The (411)A orientation is known to allow higher electron mobility and narrower photoluminescence in quantum wells (QWs).[24–26] Our own results on InGaAs/InAlAs double-QW structures lattice-matched to InP have confirmed a marked increase in the electron mobility in (411)A oriented samples[27] and have inspired us to investigate if a reduced intrasubband scattering seen in transport translates into a reduction in intersubband scattering that is detrimental to QCL operation. In this letter, we compare the intersubband scattering due to IFR scattering in lattice-matched QCLs grown on (411)A to (100) InP substrates. We show that, indeed, the QCLs grown on (411)A InP substrates have twice the power efficiency, higher slope efficiency, higher gain, and lower threshold current density compared to those with (100) orientation.

Based on the above considerations (see Fig. 1), QCLs with an emission wavelength of 9 μm are well suited to study the effect of the substrate orientation on IFR scattering. The QCL design is based on InGaAs/InAlAs heterosystem lattice-matched to InP and uses the so-called "*dual-upper-state to multiple-lower-state*" active region published by Fujita and co-authors.[28] Two QCL wafers were grown one after another using the same doping, the same waveguide structure, and the same growth temperature of 500 °C: one on the conventional (100) oriented InP substrate as a reference (our Reference Number 2-2003) and one on a (411)A oriented substrate (Reference Number 2-2025). Both wafers show sharp X-ray rocking curves with distinct satellites, which allow a good estimation of the average growth rate. Simulation of the rocking curves gives the following average layer thickness deviation from the nominal design thicknesses: +1.5% for the reference wafer grown on the (100) substrate and +2.9% for the wafer grown on the (411)A substrate. These small deviations cannot account for the substantial difference in QCL performance.[29] Reproducibility of the same active region doping level was confirmed by Hg-probe capacitance-voltage measurements. For that purpose, the top InP contact and cladding layer were removed on a piece of wafer by selective wet etching using concentrated HCl. The measurements indicate an average active region doping level of $1.4(\pm 0.2) \times 10^{16}\,\text{cm}^{-3}$ for the reference wafer grown on the (100) substrate and $1.2(\pm 0.2) \times 10^{16}\,\text{cm}^{-3}$ for the wafer grown on the (411)A substrate. These measurements of the bulk doping give a two-dimensional carrier concentration per cascade of $N_{2D} = 9.5 \times 10^{10}\,\text{cm}^{-2}$ and $8.1 \times 10^{10}\,\text{cm}^{-2}$, respectively.

The wafers were processed into ridge waveguides of approximately 30 μm width using conventional photolithography and wet chemical etching. The ridges on the (411)A substrate were oriented along the $[1\bar{1}0]$ direction, so that the ridge facets could be simply cleaved perpendicular to the laser ridge [as on (100) substrates]. The laser sidewalls were electrically insulated with SiO_2. Top contacts of Cr/Au and back contacts of AuGe/Cr/Au were thermally evaporated and annealed at 300 °C for 2 min in a 1:10 H_2:N_2 atmosphere. The top contact was additionally coated with 5 μm galvanic gold, including cleaving gaps every 2 mm. The QCLs of various lengths were cleaved, soldered on CuW submounts, and characterized in a closed-cycle cryostat at various temperatures between 60 K and 280 K in the pulsed mode (150 ns pulses, 10 kHz repetition frequency). The lasers operate also at room temperature and above; the temperature range of 60–280 K is used because our cryostat can maintain stable temperature only within this range.

Figure 2 compares the power efficiency (ratio of laser power out to electrical power in; also called wall-plug efficiency) of the QCL grown on a (411)A substrate and the reference QCL grown on a (100) InP substrate at 280 K. We observe more than a twofold increase in the maximum power efficiency due to reduced IFR scattering resulting from the use of the (411)A substrates. The scale of the power efficiency improvement varies somewhat from laser to laser but falls approximately in the range between two- and three-fold. Improved power efficiency is ultimately the motivation for this investigation but depends on several factors including threshold current density, slope efficiency, and dynamic range.[30]

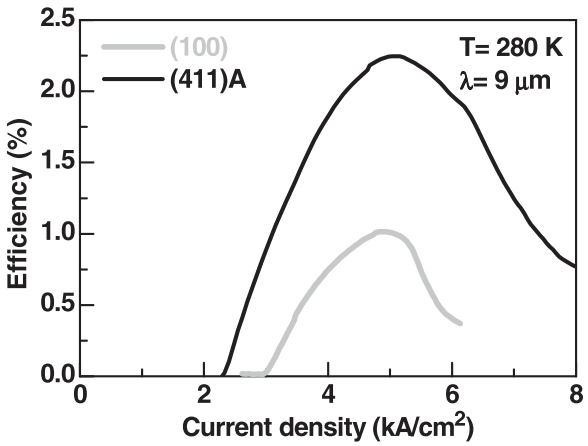

FIG. 2. Power (wall plug) efficiency as a function of the current density compared for the same QCL structures grown on (411)A and (100) oriented InP substrates as indicated. Both lasers were 4 mm long. The lasers grown on (411)A and (100) substrates had 24.4 μm and 32.7 μm wide ridges, respectively.

As seen in Fig. 3 (top panel), the threshold current density is consistently lower for the laser grown on the (411)A substrate. We attribute this improvement to reduced scattering out of the upper laser level as well as, perhaps, a narrower gain region—we were unable to measure sub-threshold electroluminescence. The (411)A advantage becomes smaller at higher temperatures due to an increasing influence of phonon scattering. Figure 3 (bottom panel) depicts the slope efficiency as a function of temperature for the QCLs grown on (411)A and (100) oriented InP substrates. For temperatures above 150 K, the slope efficiency is generally about 50% higher for the QCL grown on (411)A substrate compared to the reference QCL. At very low temperatures, the slope efficiency for the (411) QCL saturates, probably due to some freeze-out in this low-doped structure. We have also tested wider (33.2 μm) lasers processed out of the same (411)A-oriented QCL wafer. These have shown very similar temperature behavior ($T_0 = 217$ K and $T_1 = 234$ K), compared to the data of Fig. 3. Thus, differences in transient thermal effects can be neglected for such a low duty cycle of 0.15%.

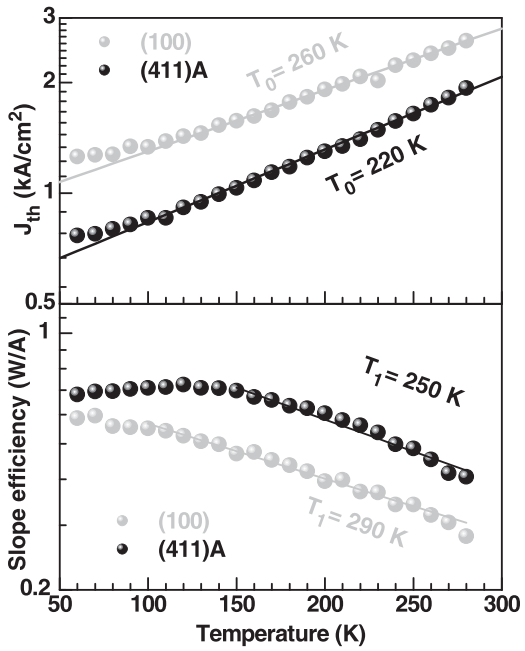

FIG. 3. Top panel: Threshold current densities as functions of temperature for otherwise identical QCL structures grown on (411)A and (100) oriented InP substrates. The lasers grown on (411)A and (100) substrates had 24.4 μm and 32.7 μm wide ridges, respectively, and were 4 mm in length. Bullets are experimental data and the lines are simple exponential fits: $J_0 \exp(T/T_0)$. Bottom panel: Slope efficiency functions of temperature for otherwise identical QCL structures grown on (411)A and (100) oriented InP substrates. The lasers grown on (411)A and (100) substrates had 24.4 μm and 32.7 μm wide ridges, respectively, and were 4 mm in length. Bullets are experimental data and the lines are simple exponential fits: $\eta_0 \exp(-T/T_1)$.

Figure 4 depicts the threshold current density for the QCLs grown on (411)A and (100) InP substrates as a function of the reciprocal cavity length and gives us the values of the waveguide loss coefficient α_w and the modal gain coefficient $g\Gamma$. Consistent with the other data, we obtain higher modal gain for the QCL grown on the off-cut substrate. On the other hand, the waveguide loss coefficient for the (411) QCL was also higher. The reason for the latter result is not clear but is probably due to differences in optical absorption within the dielectric, since the expected free carrier absorption within the active region is smaller than what is measured in either laser.

This study was motivated by the observed difference in intrasubband IFR scattering between (100) and (411) oriented structures, resulting in the (411) structures having much higher electron mobility than (100) structures.[27] In that study, a double QW structure was used to increase the overlap of the electronic wavefunction with the interface in order to emphasize the IFR scattering. Those structures were much higher doped than QCL structures—about $1 \times 10^{12}\,\mathrm{cm}^{-2}$, resulting in a relatively large Fermi wavevector k_F. For intraband scattering, the most important scattered wavevector is $q = 2k_F$, which for these structures was about $0.5\,\mathrm{nm}^{-1}$, similar to intersubband scattering for $\lambda = 9\,\mu$m. Similarly, the value of Λ relevant for PL exciton linewidth studies is also about $0.5\,\mathrm{nm}^{-1}$.[24] For this reason, all three of these experiments probe a similar lateral roughness parameter Λ. Consistent with the mobility and PL studies, the intersubband IFR scattering was significantly smaller in the (411) QCL structures compared to the (100) structures. This difference in

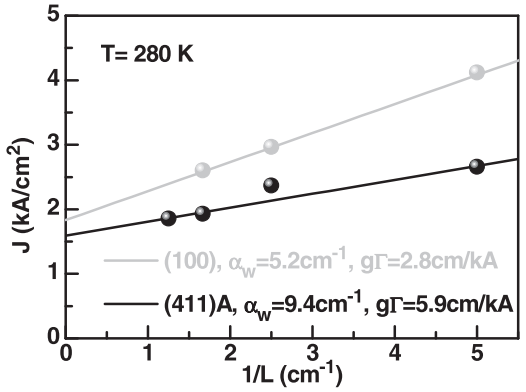

FIG. 4. Threshold current densities as functions of the reciprocal laser length for otherwise identical QCL structures grown on (411)A and (100) oriented InP substrates. Bullets are experimental data and the lines are fits, using the listed parameters of α_w and $g\Gamma$. The lasers were cleaved into 2-mm, 4-mm, 6-mm, and 8-mm long bars. The lasers grown on a (411)A substrate had 24.4 μm wide ridges, and the laser grown on a (100)A substrate had 32.7 μm wide ridges.

scattering is seen experimentally in the threshold current density, slope efficiency, and power efficiency. A reduced IFR scattering results in better inversion, longer upper laser state lifetime, smaller non-radiative recombination, and less leakage current during injection.[19]

To summarize, we have compared the performance of two nominally identical QCLs grown on (411)A and the standard (100) InP substrates. The QCL active regions are composed of InGaAs QWs and InAlAs barriers lattice-matched to InP and lase at 9 μm. The lasers grown on the (411)A substrate have shown a two- to three-fold improvement in power efficiency. Furthermore, threshold current density and slope efficiency are also better in the (411) structures. We relate this performance improvement to reduction of the electron scattering on the interface roughness, taking place in the laser grown on the (411)A substrate. In the view of these results, the use of (411)A wafers appears to be an efficient way to improve QCL efficiency. If applied to THz QCLs,[12] such an efficiency improvement could result in higher maximum operation temperatures.

This work was financially supported by German Research Society (DFG), Project No. MA_1749_22-1, by the Mid-TECH project funded by the European Union's Horizon 2020 research and innovation program under Grant Agreement No. 642661 and through COMTERA, a program under the auspices of ERA.NET RUS PLUS.

[1]J. Faist, F. Capasso, D. L. Sivco, C. Sirtori, A. L. Hutchinson, and A. Y. Cho, Science **264**, 553 (1994).
[2]L. Diehl, D. Bour, S. Corzine, J. Zhu, G. Höfler, M. Lončar, M. Troccoli, and F. Capasso, Appl. Phys. Lett. **88**, 201115 (2006).
[3]A. Wittmann, Y. Bonetti, M. Fischer, J. Faist, S. Blaser, and E. Gini, IEEE Photonics Technol. Lett. **21**, 814 (2009).
[4]Y. Bai, N. Bandyopadhyay, S. Tsao, S. Slivken, and M. Razeghi, App. Phys. Lett. **98**, 181102 (2011).
[5]A. Lyakh, M. Suttinger, R. Go, P. Figueiredo, and A. Todi, Appl. Phys. Lett. **109**, 121109 (2016).
[6]J. Faist, Appl. Phys. Lett. **90**, 253512 (2007).
[7]D. Botez, C.-C. Chang, and L. J. Mawst, J. Phys. D: Appl. Phys. **49**, 043001 (2016).
[8]W. T. Masselink, M. P. Semtsiv, A. Aleksandrova, and S. Kurlov, Opt. Eng. **57**, 011015 (2017).
[9]A. Vasanelli, A. Leuliet, C. Sirtori, A. Wade, G. Fedorov, D. Smirnov, G. Bastard, B. Vinter, M. Giovannini, and J. Faist, Appl. Phys. Lett. **89**, 172120 (2006).
[10]J. B. Khurgin, Y. Dikmelik, P. Q. Liu, A. J. Hoffman, M. D. Escarra, K. J. Franz, and C. F. Gmachl, Appl. Phys. Lett. **94**, 091101 (2009).
[11]Y. T. Chiu, Y. Dikmelik, P. Q. Liu, N. L. Aung, J. B. Khurgin, and C. F. Gmachl, Appl. Phys. Lett. **101**, 171117 (2012).
[12]K. A. Krivas, D. O. Winge, M. Francki, and A. Wacker, J. Appl. Phys. **118**, 114501 (2015).
[13]Y. V. Flores and A. Albo, IEEE J. Quantum Electron. **53**, 2300208 (2017).
[14]C. Becker, C. Sirtori, O. Drachenko, V. Rylkov, D. Smirnov, and J. Léotin, Appl. Phys. Lett. **81**, 2941 (2002).
[15]O. Drachenko, J. Galibert, J. Léotin, J. W. Tomm, M. P. Semtsiv, M. Ziegler, S. Dressler, U. Müller, and W. T. Masselink, Appl. Phys. Lett. **87**, 072104 (2005).
[16]M. P. Semtsiv, Y. Flores, M. Chashnikova, G. Monastyrskyi, and W. T. Masselink, Appl. Phys. Lett. **100**, 163502 (2012).
[17]A. Bismuto, R. Terazzi, M. Beck, and J. Faist, Appl. Phys. Lett. **98**, 091105 (2011).
[18]A. Gold, Phys. Rev. B **35**, 723 (1987).
[19]Y. V. Flores, M. P. Semtsiv, M. Elagin, G. Monastyrskyi, S. Kurlov, A. Aleksandrova, J. Kischkat, and W. T. Masselink, J. Appl. Phys. **113**, 134506 (2013).
[20]S. S. Kurlov, M. P. Semtsiv, Z. Ya. Zhuchenko, G. G. Tarasov, and W. T. Masselink, Semicond. Phys. Quantum Electron. Optoelectron. **21**, 186 (2018).
[21]S. Tsujino, A. Borak, E. Muller, M. Scheinert, C. V. Falub, H. Sigg, D. Grutzmacher, M. Giovannini, and J. Faist, Appl. Phys. Lett. **86**, 062113 (2005).
[22]A. Wittmann, Y. Bonetti, J. Faist, E. Gini, and M. Giovannini, Appl. Phys. Lett. **93**, 141103 (2008).
[23]D. Botez, J. D. Kirch, C. Boyle, K. M. Oresick, C. Sigler, H. Kim, B. B. Knipfer, J. H. Ryu, D. Lindberg III, T. Earles, L. J. Mawst, and Y. V. Flores, Opt. Mater. Express **8**, 1378 (2018).
[24]S. Shimomura, A. Wakejima, A. Adachi, Y. Okamoto, N. Sano, K. Murase, and S. Hiyamizu, Jpn. J. Appl. Phys., Part 2 **32**, L1728 (1993).
[25]I. Watanabe, K. Kanzaki, T. Kitada, M. Yamamoto, S. Shimomura, and S. Hiyamizu, J. Cryst. Growth **251**, 90 (2003).
[26]T. Kitada, T. Aoki, I. Watanabe, S. Shimomura, and S. Hiyamizu, Appl. Phys. Lett. **85**, 4043 (2004).
[27]D. Alcer, M. P. Semtsiv, and W. T. Masselink, J. Cryst. Growth **477**, 110 (2017).
[28]K. Fujita, S. Furuta, T. Dougakiuchi, A. Sugiyama, T. Edamura, and M. Yamanishi, Opt. Express **19**, 2694 (2011).
[29]The growth campaign includes variations in doping and unintended layer thickness deviation. Whereas doping plays a critical role in performance, the thickness deviations of $<3\%$ are inconsequential.
[30]The laser reported in Ref. 28 shows better performance than our reference laser. Both our (100) reference laser and our (411)A laser were grown within the same growth campaign, the only difference being the substrate orientation. Thus, the advantage of (411)A over (100) is evident.